

# Automatic Thresholding of Color Edges

*H. M. G. Stokman and Th. Gevers*  
*Intelligent Sensory Information Systems*  
*University of Amsterdam, The Netherlands*

## Abstract

Color edge information can be used to measure or recognize objects in images. False color edges introduced by noise are conventionally eliminated by thresholding. The problem is how to find such threshold value. We present and empirically verify a principled method for automatic, local determination of the threshold value. The method is based on the theoretical error propagation of photon noise through the computation of the color gradient.

## 1. INTRODUCTION

Color edge information from an image can be used to measure or recognize objects in images. The color edges correspond to significant changes in the image, ideally at the boundary between two different regions, e.g. between a foreground object and the background. False edges are often detected due to sensor noise. These false edges are conventionally eliminated by using a threshold which determines the minimum acceptable gradient modulus. The same global threshold value is typically used for all edges in an image. The problem is how to find such threshold value. Usually the value is found by trial-and-error. We therefore believe that an automatic, principled way for (local) threshold value selection is of interest for image processing tasks which use color edge information.

A number of well established techniques for edge detection in ordinary (one-band) images is available, see for instance the recent overview of Ziou and Tabbone [1]. These edge detection methods can be extended to color images by taking the sum or the root mean square of the individual edge maps, or by more principled methods described by Sapiro [2]. The edges can be thresholded by manually selecting an appropriate threshold value, or by automatically selecting the value based on the statistical properties of the gradient magnitude of the image [3]. For example, the threshold can be chosen so that only  $N\%$  of pixels in the image are classified as edges.

Burns and Berns [4] analyze the error propagation from a measured color signal to the CIE  $L^*a^*b^*$  color space to indicate how the color space transform influences the mean, variance and covariance of the color measurement. Shafarenko, Petrou and Kittler [5] use an adaptive filter for noise reduction in the 3-D color histogram in the CIE

$L^*u^*v^*$  space. The filter width depends on the covariance matrix of the noise distribution in the CIE  $L^*u^*v^*$  space. In this paper, we present and empirically verify a principled method for automatic, local determination of the threshold value. The method is based on the theoretical error propagation of photon noise through the computation of the color gradient.

The paper is organized as follows. In section (2) the equations for color space transformations and color edge detection are specified which will be used throughout the paper. In section (3) the error propagation of measurement uncertainty in  $RGB$  values to the gradient strength is analyzed. Using combined camera and sensor noise model, the uncertainty in  $RGB$  values itself is theoretically determined in section (4). Based on these results, an algorithm for automatic and local thresholding is statistically inferred in section (5). In section (6), the proposed method is empirically verified. Section (7) finishes the paper.

## 2. Transformed Colors and Color Edge Detection

Based on the measured  $RGB$  values, the normalized red and green color values  $rg$  at position  $(u, v)$  are computed as

$$r(u, v) = \frac{R(u, v)}{R(u, v) + G(u, v) + B(u, v)} \quad (1)$$

$$g(u, v) = \frac{G(u, v)}{R(u, v) + G(u, v) + B(u, v)} \quad (2)$$

The opponent colors red-green  $o$  and yellow-blue  $p$  are computed as

$$o(u, v) = \frac{R(u, v) - G(u, v)}{2} \quad (3)$$

$$p(u, v) = \frac{2B(u, v) - R(u, v) - G(u, v)}{4} \quad (4)$$

After this color transformation, the color planes of an image are differentiated in the  $u$  and  $v$  direction using the Prewitt masks

$$\begin{bmatrix} -1 & 0 & 1 \\ -1 & 0 & 1 \\ -1 & 0 & 1 \end{bmatrix} \quad \text{and} \quad \begin{bmatrix} -1 & -1 & -1 \\ 0 & 0 & 0 \\ 1 & 1 & 1 \end{bmatrix}$$

giving the gradient as  $\left(\frac{\partial c_i}{\partial x}, \frac{\partial c_i}{\partial y}\right)$ , respectively. Here,  $c_i$  is the notation for particular color planes, for instance for the opponent color space  $c_1 = o$  and  $c_2 = p$ , for the normalized color space  $c_1 = r$  and  $c_2 = g$  and for sensor space  $c_1 = R$ ,  $c_2 = G$  and  $c_3 = B$ . The Prewitt operator is adapted merely for its simplicity.

The modulus of the gradient of the color planes is obtained by taking the Euclidean distance:

$$\nabla F(u, v) = \sqrt{\sum_i \left[ \left( \frac{\partial c_i(u, v)}{\partial u} \right)^2 + \left( \frac{\partial c_i(u, v)}{\partial v} \right)^2 \right]} \quad (5)$$

In the next section, the error propagation of measurement uncertainty in  $RGB$  values to the gradient strength is analyzed.

### 3. Error Propagation of Measurement Uncertainty

It is common practice to state the result  $\hat{g}$  of a series of measurements of a quantity  $x$  as

$$\hat{g}(x) = x_{\text{best}} \pm \sigma_x \quad (6)$$

where  $x_{\text{best}}$  is the best estimate for the quantity  $x$  (e.g. the average value) and  $\sigma_x$  is the uncertainty in the measurement of  $x$  (e.g. the standard deviation). Suppose that  $x, \dots, z$  are measured with corresponding uncertainties  $\sigma_x, \dots, \sigma_z$ , and the measured values are used to compute the function  $q(x, \dots, z)$ . If the uncertainties in  $x, \dots, z$  are independent, random and relatively small, then the predicted uncertainty in  $q$  [6] is

$$\sigma_q = \sqrt{\left( \frac{\partial q}{\partial x} \sigma_x \right)^2 + \dots + \left( \frac{\partial q}{\partial z} \sigma_z \right)^2} \quad (7)$$

where  $\partial q/\partial x$  and  $\partial q/\partial z$  are the partial derivatives of  $q$  with respect to  $x$  and  $z$ . In any case, the uncertainty in  $q$  is never larger than

$$\sigma_q \leq \left| \frac{\partial q}{\partial x} \right| \sigma_x + \dots + \left| \frac{\partial q}{\partial z} \right| \sigma_z \quad (8)$$

The uncertainty of the normalized coordinates is found by substitution of (1) and (2) into (7), see (9) and (10). Here,  $\sigma_R, \sigma_G$  and  $\sigma_B$  denote the uncertainty associated with  $R, G$  and  $B$ , and  $\sigma_r$  and  $\sigma_g$  represent the uncertainty in the normalized red and green color components, respectively. Similarly the uncertainty of the opponent coordinates is found by substitution of (3) and (4) into (7) as

$$\sigma_o(u, v) = \frac{1}{2} \sqrt{\sigma_G(u, v)^2 + \sigma_R(u, v)^2} \quad (11)$$

$$\sigma_p(u, v) = \frac{1}{2} \sqrt{4\sigma_B(u, v)^2 + \sigma_G(u, v)^2 + \sigma_R(u, v)^2} \quad (12)$$

The transformed color components are dependent, e.g. uncertainties that occur in the  $R$  channel effect both the red-green and yellow-blue components of the opponent colors. To propagate the uncertainties from these color components to the gradient modulus, the uncertainties are therefore determined using (8). To analyze the error propagation due to filtering, first consider (7). From (7) it follows that if a color  $x$  is measured with uncertainty  $\sigma_x$  and if it is used to compute the product  $q = Bx$  where  $B$  has no uncertainty, then uncertainty  $q$  is  $\sigma_q = |B|\sigma_x$ . For the Prewitt filter,  $|B|$  attains the value 1. From (8) it follows that if  $x, \dots, w$  are determined with uncertainties  $\sigma_x, \dots, \sigma_w$  and if these values are used to compute  $q = Bx + \dots + Bw$ , then  $\sigma_q$  is never larger than their ordinary sum  $\sigma_q \leq |B|\sigma_x + \dots + |B|\sigma_w$ . Consequently, the propagation of uncertainty of the Prewitt filter can be implemented by filtering the uncertainty planes of the different color spaces with the masks

$$\begin{array}{|c|c|c|} \hline 1 & 0 & 1 \\ \hline 1 & 0 & 1 \\ \hline 1 & 0 & 1 \\ \hline \end{array} \quad \text{and} \quad \begin{array}{|c|c|c|} \hline 1 & 1 & 1 \\ \hline 0 & 0 & 0 \\ \hline 1 & 1 & 1 \\ \hline \end{array}$$

which gives the uncertainties in the gradient  $\sigma_{\partial c/\partial u}$  and  $\sigma_{\partial c/\partial v}$ , respectively.

The uncertainty in the gradient modulus of (5) is determined by (8), see (13). This way, the transformed color uncertainty is propagated to the computation of the color gradient.

### 4. Camera and Noise Models

To explain a measured pixel value, we use a polynomial camera model

$$i(u, v) = gh(u, v) + d(u, v) \quad (14)$$

$i$  denotes the output signal at position  $(u, v)$ ,  $h$  the input signal,  $d$  the dark current,  $g$  the gain. Modern CCD cameras are sensitive enough to be able to count individual photons. Photon noise arises from the fundamentally stochastic nature of photon production. The probability distribution for counting  $\rho$  events (here: photons) during  $t$  seconds is known to be Poisson. The number of photons measured is given by its average as

$$h(u, v) = \rho t \pm \sqrt{\rho t} \quad (15)$$

Let  $\sigma_d$  denote the dark current uncertainty. Incorporating  $\sigma_d$  and the uncertainty of (15) in (14) gives

$$i(u, v) \pm \sigma_{i(u, v)} = g[\rho t \pm \sqrt{\rho t}] + [d(u, v) \pm \sigma_d] \quad (16)$$

$$\sigma_r(u, v) = \sqrt{\frac{R(u, v)^2[\sigma_B(u, v)^2 + \sigma_G(u, v)^2] + [B(u, v) + G(u, v)]^2\sigma_R(u, v)^2}{[B(u, v) + G(u, v) + R(u, v)]^4}} \quad (9)$$

$$\sigma_g(u, v) = \sqrt{\frac{G(u, v)^2[\sigma_B(u, v)^2 + \sigma_R(u, v)^2] + [B(u, v) + R(u, v)]^2\sigma_G(u, v)^2}{[B(u, v) + G(u, v) + R(u, v)]^4}} \quad (10)$$

Dark current compensation is performed either by software or internally in the camera. Subtraction of a constant value  $c$  such that  $d(x, y) = c$  from the image removes the dark current, but not the dark current uncertainty:

$$[i(u, v) - c] \pm \sigma_{i(u, v)} = g\rho t \pm (g\sqrt{\rho t} + \sigma_d) \quad (17)$$

An extension of this model for a dark current compensated color camera with  $n$  color channels,  $n \in \{R, G, B\}$ , is

$$i(u, v)_n \pm \sigma_{i(u, v), n} = g_n \rho_n t \pm (g_n \sqrt{\rho_n t} + \sigma_d) \quad (18)$$

Our interest is to predict  $\sigma_{i(u, v), n}$ . Let the average image intensity measured over a homogeneously colored patch be denoted  $I = g\rho t$ , the associated variance  $\text{var}(I) = g^2 \rho t$  and the dark current variance  $\text{var}(d) = \sigma_d^2$ . We now have the linear relation between  $I$  and  $\text{var}(I)$  based on [7] as

$$\text{var}(I) = gI + \text{var}(d) \quad (19)$$

which is of the general form  $y = ax + b$ . For (18) we obtain

$$\text{var}(I_n) = g_n I_n + \text{var}(d) \quad (20)$$

If measurements are made of the image intensity and corresponding image variance, then the values of  $\text{var}(d)$ ,  $g_R$ ,  $g_G$ ,  $g_B$  are obtained by linear regression.

Let  $\text{var}(I_{n, k})$  denote the  $k$ th of  $N$  measurements of the variance of the  $n$ th color channel and let  $I_{n, k}$  denote the corresponding average intensity. Ordering these measurements as equation (21) gives an over determined system allowing robust computation of the values of  $\text{var}(d)$ ,  $g_R$ ,  $g_G$ ,  $g_B$  by linear regression. Substituting these values in (20) predicts the uncertainty in a measured color value.

## 5. Thresholding of Color Edges

From (13) the uncertainty associated with the gradient modulus is known. Color edges are thresholded taking this uncertainty into account. Consider that the gradient modulus is computed for a homogeneously colored patch. These modulus values will all be approximately equal to zero. Each gradient modulus  $\nabla F(u, v)$  has an associated uncertainty  $\sigma_{\nabla F}(u, v)$ . Since the patch is homogeneously colored, the individual uncertainties  $\sigma_{\nabla F}(u, v)$  have all approximately equal values. In most experiments, if the

number of measurements is increased, the distribution of the measurements begins to take on some definite shape. The limiting distribution for measuring photons using a CCD camera is known to be Poisson. If the average number of counts is large, then the Poisson distribution is well-approximated by the Gauss distribution [6]. For a Gaussian distribution 99% of the values fall within a  $3\sigma$  margin. If a gradient modulus would be detected which exceeds  $3\sigma_{\nabla F}$  we assume that there is 1% chance that this gradient modulus corresponds to no color transition. Thus, given a gradient modulus and its associated uncertainty, we propose to assign this gradient as a color transition if the gradient modulus exceeds  $3\sigma_{\nabla}$ :

$$\nabla C(u, v) = \begin{cases} 1 & \text{if } \nabla F(u, v) > 3\sigma_{\nabla F}(u, v) \\ 0 & \text{otherwise} \end{cases} \quad (22)$$

Note that the method is essentially different from classical edge thresholding techniques where a *global* threshold value is found by a e.g. trial-and-error procedure. In contrast, (22) derives a *local* threshold value.

Consider two simple examples to clarify this. Suppose that two neighboring pixels have normalized red values of 180 and 200 and that the uncertainty associated with these values is equal and  $\sigma = 1$ , say. Suppose that the gradient modulus is simply computed as the difference between the two values and so  $\nabla F = 20$ , and that the uncertainty is computed by summation and thus  $\sigma_{\nabla F} = 2$ . Since in this example  $\nabla F > 3\sigma_{\nabla F}$  the gradient is classified as an edge. Secondly, suppose that due to low intensity one of the color values has  $\sigma = 20$ . The gradient modulus is still  $\nabla F = 20$  but this time the associated uncertainty is  $\sigma_{\nabla F} = 21$ . As in this example  $\nabla F < 3\sigma_{\nabla F}$  the gradient is *not* classified as an edge. The examples show that if color values are detected with a high uncertainty, there is a lesser probability that the gradient is classified as an edge than if the colors are detected with a low uncertainty.

## 6. Experiments

The experiments are performed using a Sony 3CCD color camera XC-003P, Matrox Corona Frame-grabber, and four Osram 18 Watt "Lumilux deLuxe daylight" fluorescent light sources.

$$\sigma_{\nabla}(u, v) \leq \frac{\sum_i \{[\partial c_i(u, v)/\partial u] \cdot \sigma_{\partial c_i/\partial u}(u, v) + [\partial c_i(u, v)/\partial v] \cdot \sigma_{\partial c_i/\partial v}(u, v)\}}{\sqrt{\sum_i \{[\partial c_i(u, v)/\partial u]^2 + [\partial c_i(u, v)/\partial v]^2\}}} \quad (13)$$

$$\begin{pmatrix} \text{var}(I_{R,1}) \\ \vdots \\ \text{var}(I_{R,N}) \\ \text{var}(I_{G,1}) \\ \vdots \\ \text{var}(I_{G,N}) \\ \text{var}(I_{B,1}) \\ \vdots \\ \text{var}(I_{B,N}) \end{pmatrix} = \begin{pmatrix} 1 & I_{R,1} & 0 & 0 \\ \vdots & \vdots & \vdots & \vdots \\ \vdots & I_{R,N} & 0 & \vdots \\ \vdots & 0 & I_{G,1} & \vdots \\ \vdots & \vdots & \vdots & \vdots \\ \vdots & \vdots & I_{G,N} & 0 \\ \vdots & \vdots & 0 & I_{B,1} \\ \vdots & \vdots & \vdots & \vdots \\ 1 & 0 & 0 & I_{B,N} \end{pmatrix} \begin{pmatrix} \text{var}(d) \\ g_R \\ g_G \\ g_B \end{pmatrix} \quad (21)$$

### 6.1. Estimation of Gain and Dark Current Uncertainty

26 images are taken of a white reference while varying the lens aperture such that each image has a different intensity as shown in figure (1). Another image is taken with a closed camera cap to establish the dark current. Goal of the experiment is to estimate the values of the gain parameters and the value of the dark current variance (20). The measured dark current is  $0.5 \pm 0.5$ . Because of this low value for both the dark current and standard deviation  $\sigma_d$ , it is assumed that the dark current is suppressed internally in the camera and therefore the obtained  $\sigma_d$  is unreliable. Instead, the  $\sigma_d$  will be estimated from the series of intensity images.

Fitting three lines through a common origin yield an electronic gain of  $g_R = 0.040$ , of  $g_G = 0.014$ , of  $g_B = 0.021$  and  $\sigma_d^2 = 2.7$ . As an indicator of how well the variance and intensity fit a straight line consider the correlation coefficient  $r$ . For the red channel,  $r = 0.995$ , for green  $r = 0.990$  and for blue  $r = 0.984$ . Since these values are close to 1, it is empirically verified that there exists a linear relation between the measured variance and the average image intensity and thus (20) is valid. The experiment shows how the parameters for the dark current and the gain are estimated for a photon limited camera system.

### 6.2. Thresholding of Color Edges

For the experiment, an image is taken of two homogeneously colored red and green plastic toys against a blue paper background. The scene is shown in fig. (2a). The red object shows two circles enclosing a number of small specularities. A homogeneous, almost black, region is visible at the right hand side of the green toy which is caused by shading. The edge map computed in the normalized

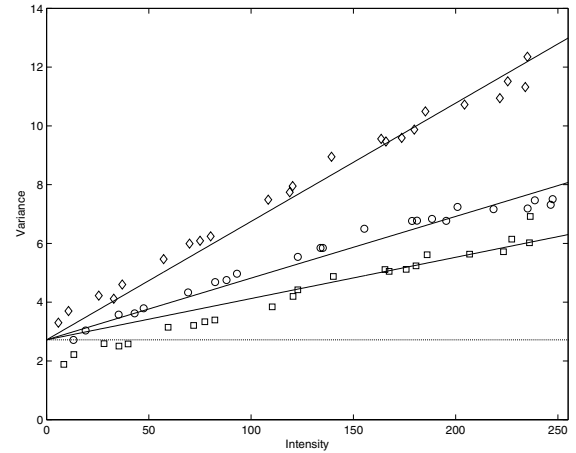


Figure 1: Visualization of the fitted lines  $\text{var}(I_n) = g_n I_n + \sigma_d^2$ . Diamonds correspond to the red color channel, squares to green and circles to blue.

color space is shown in fig. (2b). The normalized color is sensitive to highlights, and as a result the specularities at the red object show up in the edge map. The normalized color space is sensitive to noise for dark colors which can be seen in fig. (2c) which depicts the uncertainty map of the gradient modulus. The bright regions which correspond to high  $\sigma_{\nabla}$  values occur in the dark, shaded regions. As a result, many edges appear in the shaded region next to the green object of fig. (2c). In the image shown in fig. (2d), the normalized edge map is thresholded using a global threshold value. As the result shows, the specularities on the red cup have gradient moduli below the threshold value, whereas the noise edges in the shaded region have gradient moduli values which exceed the threshold

value. The experiment shows the inappropriateness of the use of a *global* threshold due to the instability of normalized colors for low intensity color values.

The result of *automatic* and *local* thresholding is shown in fig. (3a) for the gradient computed in sensor space. The image shows that many false edges are correctly suppressed while edges caused by material, geometry and specular transitions are retained. Fig. (3b) shows the result of the experiment for normalized color space. Here, automatic local thresholding correctly discards the edges present in the edge map of fig. (2b) while retaining the highlight edges on the bottom of the red cup. Note that the color transition on the right of the square box is too weak to be classified as an edge due to the neighboring region which has highly uncertain normalized color values. Fig. (3c) shows the result of automatic local thresholding for opponent color space. As expected, the color space is invariant for highlights, which consequently do not show up in the edge map.

The experiment is repeated for the image shown in fig. (4a). The result of automatic local thresholding is shown in fig. (4b-d).

## 7. Summary

In this paper, we analyzed in theory the effect of the propagation of signal dependent sensor noise through the computation of the gradient modulus in sensor, normalized and opponent color spaces. Combining the results, an edge detector was derived which *automatically* and *locally* discards false edges. The proposed method was empirically verified on homogeneously colored objects placed against a paper background.

## 8. References

1. D. Ziou and S. Tabbone. Edge detection techniques - an overview. *Pattern Recognition and Image Analysis*, 8(4):537–559, 1998.
2. G. Sapiro and D. L. Ringach. Anisotropic diffusion of multivalued images with applications to color filtering. *IEEE Transactions on Pattern Analysis and Machine Intelligence*, 5(11):1582–1586, 1996.
3. S. J. Sangwine and R. E. N. Horne, editors. *The Colour Image Processing Handbook*. Chapman & Hall, 1998.
4. P. D. Burns and R. S. Berns. Error propagation analysis in color measurement and imaging. *Color Research Applications*, 22(4), August 1997.
5. L. Shafarenko, M. Petrou, and J. Kittler. Histogram-based segmentation in a perceptually uniform color space. *IEEE Transactions on Image Processing*, 7(9):1354–1358, September 1998.
6. J. R. Taylor. *An Introduction to Error Analysis*. University Science Books, Mill Valley, CA, 1982.
7. J. C. Mullikin, L. J. van Vliet, H. Netten, F. R. Boddeke, G. van der Feltz, and I. T. Young. Methods for ccd camera characterization. In H. C. Titus and A. Waks, editors, *Image Acquisition and Scientific Imaging Systems*, volume 2173, pages 73–84. SPIE, 1994.

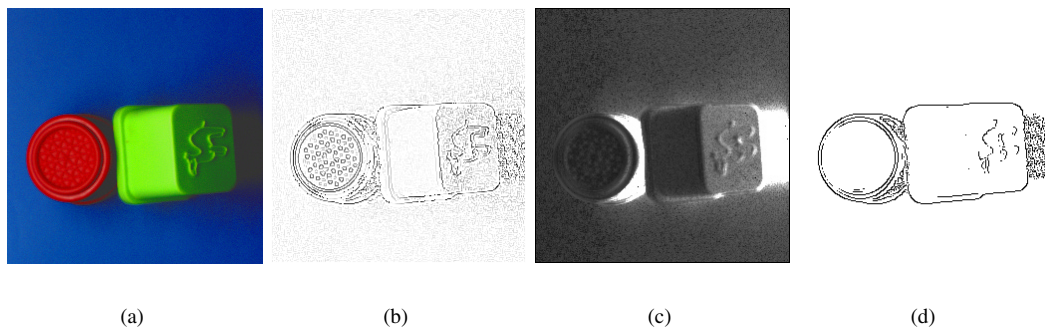


Figure 2: Edges in normalized (b) color space, and the associated uncertainty (c). In (d), the result of manual global thresholding.

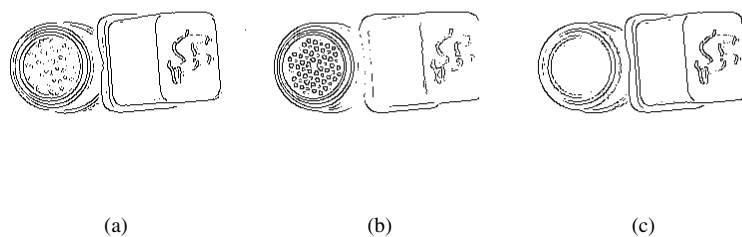


Figure 3: Results of automatic local thresholding in sensor (a), normalized (b) and opponent (c) color space.

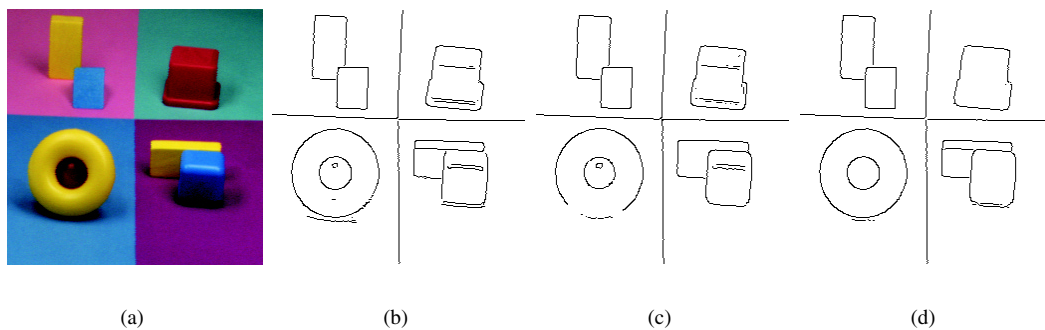


Figure 4: Results of automatic local thresholding in sensor (b), normalized (c) and opponent (d) color space.